

Bose-Einstein Condensation of Magnons in Cs_2CuCl_4

T. Radu¹, H. Wilhelm¹, V. Yushankhai^{1,2}, D. Kovrizhin³, R. Coldea⁴, Z. Tyliczynski⁵, T. Lühmann¹, and F. Steglich¹

¹Max-Planck-Institut für Chemische Physik fester Stoffe, Nothnitzer Str. 40, 01187 Dresden, Germany

²Laboratory of Theoretical Physics, JINR, 141980 Dubna, Russia

³Max-Planck-Institut für Physik komplexer Systeme, Nothnitzer Str. 38, 01187 Dresden, Germany

⁴Oxford Physics, Clarendon Laboratory, Parks Road, Oxford OX1 3PU, Great Britain

⁵Institute of Physics, Adam Mickiewicz University, Umultowska 85, 61-614 Poznań, Poland

We report on results of specific heat measurements on single crystals of the frustrated quasi-2D spin-1=2 antiferromagnet Cs_2CuCl_4 ($T_N = 0.595$ K) in external magnetic fields $B < 12$ T and for temperatures $T > 30$ mK. Decreasing B from high fields leads to the closure of the field-induced gap in the magnon spectrum at a critical field $B_c \approx 8.5$ T and a magnetic phase transition is clearly seen below B_c . In the vicinity to B_c , the phase transition boundary is well described by the power-law $T_c(B) / (B_c - B)^{1/5}$ with the measured critical exponent ≈ 1.5 . These findings are interpreted as a Bose-Einstein condensation of magnons.

PACS numbers: 75.40.-s, 75.30.Kz, 75.45.+j, 03.75.Nt

In a quantum antiferromagnet (AFM) a fully spin-polarized state can be reached at high magnetic field B exceeding a saturation field B_c . In this state, spin excitations are gapped ferromagnetic magnons. With decreasing B and passing through B_c , an antiferromagnetic long-range order of the transverse spin component develops. Provided the symmetry of the spin Hamiltonian is such that the rotational invariance around the applied field is preserved, the transverse spin component ordering can be regarded as a Bose-Einstein condensation (BEC) in a dilute gas of magnons. This concept was formulated theoretically many years ago [1, 2]. For most of the known AFMs, B_c can be well above 100 T. An exceptionally low and easily accessible saturation field of $B_c \approx 8.5$ T, however, is needed in the quantum spin-1/2 AFM Cs_2CuCl_4 . In this system the dominant exchange spin coupling J is rather weak, $J = 4.34(6)$ K [3]. The other isotropic spin coupling constants and the anisotropic Dzyaloshinsky-Moriya (DM) interaction are smaller and were determined with high accuracy by neutron experiments [4]. Thus, the spin Hamiltonian involves the isotropic exchange H_0 , the DM anisotropic term H_{DM} and the Zeeman energy H_B and is given by $H = H_0 + H_{DM} + H_B$.

Cs_2CuCl_4 falls into the class of easy-plane AFMs with U(1)-rotational invariance around the crystallographic a -axis. Thus, for B applied along the a -axis, the U(1) symmetry can be broken spontaneously due to the transverse spin component ordering at T_c . This is accompanied by the appearance of a Goldstone mode with linear dispersion, which is interpreted as signature of a magnon BEC [4]. However, an unambiguous evidence for a BEC description of the field-induced phase transition would be the determination of the critical exponent in the field dependence of the critical temperature

$$T_c(B) / (B_c - B)^{1/5} : \quad (1)$$

Theory for a 3D Bose gas predicts a universal value $\beta_{BEC} = 3/2$ [5], which coincides with the result of a mean-field treatment [6].

A magnon BEC in TiCuCl_3 was recently reported [6, 7]. In this quantum AFM with a dimerized spin-liquid ground state, the saturation field is rather high, $B_{c/2} \approx 60$ T, and the BEC transition was studied near the first critical field, $B_{c/1} \approx 5.6$ T. At $B = B_{c/1}$, the singlet-triplet excitation gap is expected to close and a BEC occurs for $B > B_{c/1}$ [6]. However, a few experimental findings show deviations from a pure magnon BEC: An anisotropic spin coupling (of unknown nature) might produce a small but finite spin gap in the ordered state for $B > B_{c/1}$ [8] and the reported critical exponent is somewhat larger than predicted by theory [6].

In this Letter we report on specific heat measurements [9] on single crystals of Cs_2CuCl_4 at low temperatures ($30 \text{ mK} < T < 6 \text{ K}$) and high magnetic fields ($B < 12 \text{ T}$) applied along the crystallographic a -axis. The aim of this thermodynamic study was (i) to trace the field dependence of $T_c(B)$ near B_c , i.e., to extract the power law according to eq. 1, and (ii) to determine the closure of the spin gap. The access to very low temperatures ($T = J \approx 10^{-2}$) enabled us to be as close as possible to the asymptotic regime where universal scaling laws are expected to hold.

Figure 1 shows the specific heat of Cs_2CuCl_4 in zero magnetic field. The magnetic contribution, C_{mag} , to the total specific heat, C_{tot} , was obtained by subtracting the phonon contribution $C_{ph} = 13599 (T/T_D)^3 \text{ J mol}^{-1} \text{ K}^{-1}$ (using a Debye temperature $T_D = 126 \text{ K}$). Furthermore, the contribution of the nuclear specific heat to the total specific heat at very low temperatures has been accounted for in the analysis of all the raw data shown in the following [10, 11]. The two prominent features present in $C(T)$ are the broad maximum related to the cross-over from the paramagnetic to a short-range spin correlated state and the λ -like peak. The latter is the signature of the entrance into the 3D magnetically ordered state ($T_N = 0.595 \text{ K}$), where the magnetic structure is a spiral in the (b,c) plane [3]. The overall shape of $C(T)$ above T_N is already captured quantitatively by including only the strongest term in the Hamiltonian,

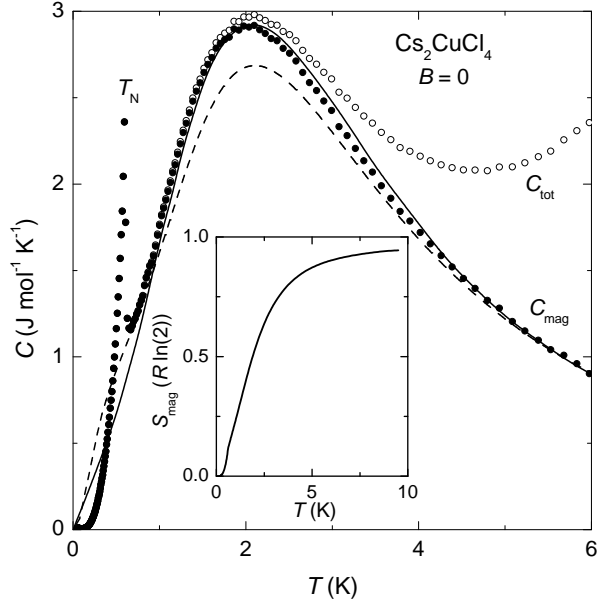


FIG. 1: Specific heat of Cs_2CuCl_4 in zero magnetic field. From the total specific heat, C_{tot} (open symbols) the phonon contribution C_{ph} has been subtracted to obtain the magnetic part C_{mag} (filled symbols). The solid and dashed lines represent the calculated $C(T)$ (see text). Inset: Temperature dependence of the magnetic entropy, $S_{\text{mag}}(T)$.

the dominant coupling J (solid line) [12]. Exact theoretical predictions are not available for the full Hamiltonian in Cs_2CuCl_4 , but including the next order term, the frustrated 2D zig-zag coupling $J^0 = J/3$, and using a high-temperature series expansion technique [13], give similar behavior (dashed line) although with a slightly lower specific heat at the position of the broad maximum. It may be possible that including the other small terms like the DM interaction ($D_a = J/5$) could improve the agreement. The magnetic entropy $S_{\text{mag}}(T)$ shows that $S = R \ln 2$ for spin-1/2 is almost recovered at 10 K (inset to Fig. 1) which corresponds roughly to the observed bandwidth of the spin excitations at base temperature [14].

The ordering temperature and the position of the broad maximum hardly change for small fields. However, the transition temperature to the spiral ordered state, which can be regarded as a cone-like structure [4], varies very strongly above 8 T (Fig. 2). Instead of T_N , we label the transition temperature in this field range T_c , as in eq. 1, in order to follow the nomenclature used in the theoretical description. The λ -like anomaly in $C_{\text{mag}}(T)$ is gradually suppressed in its height and its position is pushed to lower temperatures with increasing field. An extraordinary change occurs as the field is increased from 8.4 T to 8.44 T (inset to Fig. 2). Upon this tiny field change ($\Delta B = 0.04$ T), T_c is reduced by almost a factor of two ($T_c = 76$ mK at $B = 8.44$ T), and T_c has shifted downwards by almost one order of magnitude compared to the zero-field value. No further signatures of the tran-

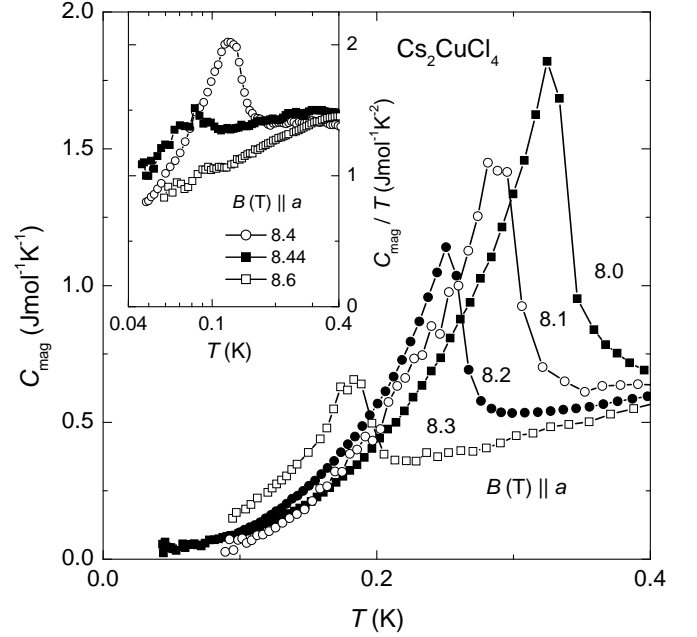


FIG. 2: Magnetic specific heat, C_{mag} vs T of Cs_2CuCl_4 close to the critical field. Inset: C_{mag}/T vs T in a semi-logarithmic plot. The data recorded at $B = 8.44$ T reveal a small jump at $T_c = 76$ mK, indicating the vicinity of the critical field.

sition can be resolved in our data upon approaching the critical field $B_c' = 8.5$ T. For $B > B_c$ the ordering of the transverse component of the magnetic moment completely disappears since the spin system enters a field-induced ferromagnetic (FM) state [4].

A field-induced gap in the magnon excitation spectrum was observed in the FM state by neutron scattering measurements [4]. Its field dependence was given to be $\Delta = g_B(B - B_c)$, with $B_c' = 8.44$ T, $g = 2.18$, and B_c the Bohr magneton. For the interpretation of the phase transition below B_c as a BEC of magnons it is crucial that the gap closes at B_c . To provide a compelling evidence for this fact we re-examined the phase diagram [4] above B_c with our thermodynamic measurements. The results are presented in Fig. 3.

The magnon dispersion along the a -direction is small due to a weak interlayer spin coupling. Thus, for temperatures well above a characteristic energy scale $E \approx 50$ mK, the actual magnon dispersion is of 2D character. However, for $T \lesssim E$ a smooth cross-over to a 3D character is expected. Assuming first a 2D quadratic magnon dispersion, the leading contribution to the temperature dependence of the specific heat is given by $C_{\text{mag}} \propto \exp(-\Delta/T) = T^2$, provided that $T < \Delta$. As shown in Fig. 3, this behavior fits well the experimental data above 0.3 K. The obtained field dependence of $\Delta(B)$ is discussed below. The deviation from a straight line of the 9 T data below 0.3 K in Fig. 3 might indicate the cross-over from 2D to 3D magnons. This notion is supported by the low-temperature data plotted as C_{mag}/T^2 vs $1/T$ in the inset to Fig. 3. This presentation is used

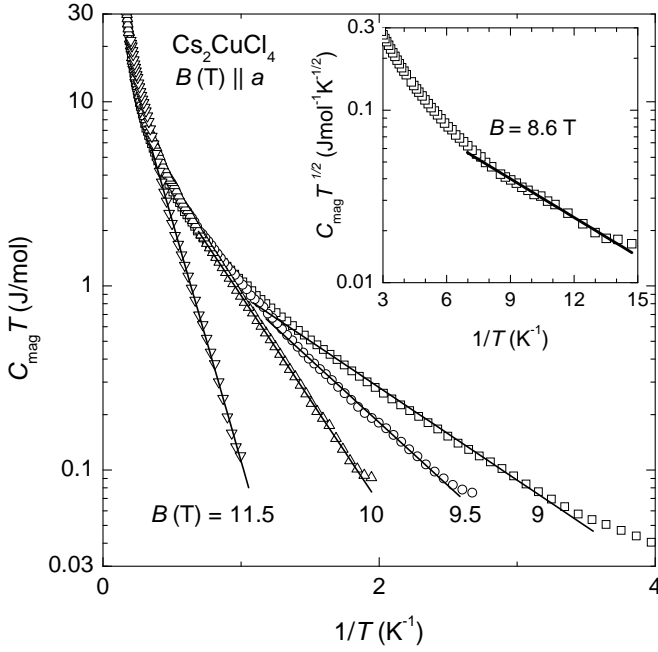


FIG. 3: Semi-logarithmic plot of $C_{\text{mag}} T$ vs $1/T$ of Cs_2CuCl_4 for fields above B_c . In this representation the slope of the data (solid lines) yields the value of the gap present in the magnon excitation spectrum. The data shown in the inset were obtained at $B = 8.6$ T and are plotted as $C_{\text{mag}} T^{1/2}$ vs $1/T$.

since a 3D dispersion relation yields as leading term in the specific heat $C_{\text{mag}} \propto \exp(-\Delta/T) = T$. The straight line below 0.15 K indicates that this model describes the data appropriately. However, in this cross-over region, the 2D model describes the data equally well and the determined value of the gap is (within the error bar) the same as the one deduced from the $C_{\text{mag}} T$ vs $1/T$ plot.

The $(T; B)$ phase diagram of Cs_2CuCl_4 obtained from our specific heat experiments is presented in Fig. 4. The field dependence of the magnetic transition temperature is in very good agreement with $T_c(B)$ obtained from neutron data up to 8 T [14]. The specific heat data, however, revealed that T_c starts to decrease strongly above 8 T and $T_c \rightarrow 0$ for $B \rightarrow B_c$. Fitting the power law dependence $T_c(B) / (B_c - B)^g$ to the data for $B \rightarrow 8$ T with the assumption of $B_c = 8.50$ T yields an exponent $g = 1.52(10)$. We want to stress that the value of g is very sensitive to the chosen value of B_c . An exponent $g = 1.44(10)$ is obtained if $B_c = 8.51$ is used. The solid line plotted in the inset to Fig. 4 represents the result of the theoretical analysis described below. Above B_c the fully spin-polarized FM state is created and the gap opens in the spin excitation spectrum. The dashed line represents a linear fit to the data for $B \rightarrow 10$ T (main part of Fig. 4). This yields $B_c = 8.3(10)$ T and $g = 2.31(15)$. The relatively large errors are due to the uncertainties in the fit.

To treat the observed phase transition slightly below

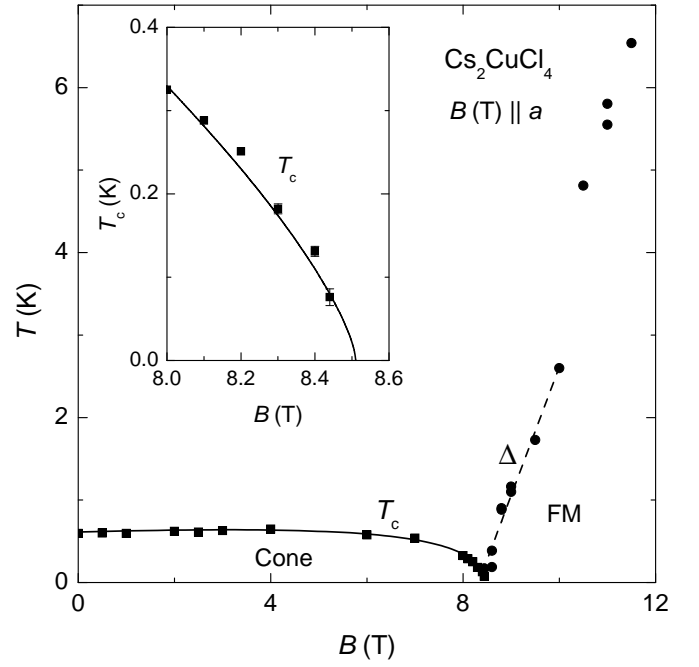


FIG. 4: $(T; B)$ phase diagram of Cs_2CuCl_4 for $B \parallel a$. The ordering temperature T_c decreases as the magnetic field approaches the critical field $B_c = 8.51$ T. Above B_c a field-polarized ferromagnetic (FM) state is entered and the gap in the spin excitation spectrum opens. Inset: The experimental $T_c(B)$ data points are well described by the calculated phase boundary of the BEC of magnons (solid line).

the saturation field B_c as a BEC of magnons [1, 2, 6] we used the hard-core boson representation for spin-1=2 operators $S_i^x; S_i^z$ in the original Hamiltonian H . Because the DM interaction ($D = 0.053(5)$ J [4]) changes sign between even and odd magnetic layers, which are stacked along the a -direction, two types of bosons, a_i and b_j are introduced for the two types of layers [15, 16]. The hard-core boson constraint was satisfied by adding to H an infinite on-site repulsion, $U \rightarrow \infty$, between bosons given by

$$H_U^{(a)} + H_U^{(b)} = U \sum_i a_i^\dagger a_i^\dagger a_i a_i + U \sum_j b_j^\dagger b_j^\dagger b_j b_j; \quad (2)$$

The interlayer coupling $J^0 = 0.045(5)$ J [4] mixes a and b boson modes and results in two bare magnon excitation branches A and B. Their dispersion relations are given by [4]

$$E_q^{A/B} = J_q \frac{q}{\sqrt{D_q^2 + J_q^0}} E_0; \quad (3)$$

with

$$J_q = J \cos q_x + 2J^0 \cos(q_x/2) \cos(q_y/2); \quad (4)$$

$$D_q = 2D \sin(q_x/2) \cos(q_y/2); \quad (5)$$

$$J_q^0 = J^0 \cos(q_z/2); \quad (6)$$

Here $J^0 = 0.34(3)J$ [4] and the q -values are restricted to $0.6 q_x < 2$, $0.6 q_y < 4$, and $0.6 q_z < 2$.

The degenerate minima $E_{Q_1}^A = E_{Q_2}^B = 0$ are at $Q_1 = (1; 0; 0)$ for branch A and at $Q_2 = (2; 2; 0)$ for branch B. Without losing precision we can use $Q_1' = Q_2' = 2 \arcsin(J^0/2J)$. The bilinear part of H now reads

$$H_{\text{bil}} = \sum_q E_q^A a_q^\dagger a_q + E_q^B b_q^\dagger b_q; \quad (7)$$

with $A_q = a_q a_q + b_q b_q$, $B_q = a_q b_q + b_q a_q$, $\frac{1}{2} + \frac{1}{2} = 1$, and the bare chemical potential $\mu_0 = g_B(B_c - B)$. The saturation field $B_c = W/(g_B)$, with W being the magnon bandwidth, was calculated to be $B_c = 8.51$ T assuming $g = 2.20$ [16, 17].

The interaction given by eq. 2 describes the scattering of A and B magnons. Near the quantum critical point, $(B_c - B) \ll B_c$ and at low temperature, the average density of magnons $n^A = n^B = n$ is low, $n \ll (1 - B/B_c)$. The magnon scattering can be treated in the ladder approximation [18], neglecting interference between a and b channels. In this approximation, the problem reduces to solving the Bethe-Salpeter equation in each channel.

This results in the renormalized scattering amplitudes $(i) (\mathbf{q}_1; \mathbf{q}_2; \mathbf{q}_3; \mathbf{q}_4)$ for $i = a, b$. Here $\mathbf{q}_3; \mathbf{q}_4$ and $\mathbf{q}_1; \mathbf{q}_2$ are magnon momenta before and after scattering, respectively, and $\mathbf{q}_1 + \mathbf{q}_2 = \mathbf{q}_3 + \mathbf{q}_4$. The total energy of scattered magnons was set to zero. This limit is compatible with our main goal to describe the phase transition near B_c when approaching the phase boundary $T_c(B)$ from higher temperatures. At $T \ll T_c$, only the magnon states at $q' = Q_{1,2}$ are occupied and the magnon spectrum renormalization near the minimum is important.

With given (a) and (b) , the complete set of two-particle scattering amplitudes was then obtained by multiplying $(a); (b)$ by products of four q and q coefficients. For instance, a scattering process $(A_{\mathbf{q}_3}; B_{\mathbf{q}_4}) \rightarrow (A_{\mathbf{q}_1}; B_{\mathbf{q}_2})$ in the channel a is described by the amplitude $q_1 q_2 q_3 q_4 (a) (\mathbf{q}_1; \mathbf{q}_2; \mathbf{q}_3; \mathbf{q}_4)$.

The renormalization of low-energy magnons was found by treating the magnon scattering effects in the Hartree-Fock approximation:

$$H_{\text{int}}^{\text{MF}} = 2n \sum_q A_q^\dagger A_q + B_q^\dagger B_q + 2 \mu_0 n \sum_q A_q^\dagger B_q + B_q^\dagger A_q; \quad (8)$$

where $\frac{1}{Q_1} = \frac{1}{Q_2} = 2$ and $\frac{1}{Q_1} = \frac{1}{Q_2} = 2$. Taking

into account that $\frac{1}{Q_1} = \frac{1}{Q_2} = 2$, we keep here only the leading contributions to energy parameters μ_0 and μ_0' :

$$\begin{aligned} \mu_0 &= 4 (a) Q_1; Q_1; Q_1; Q_1 \\ &= 4 (b) Q_2; Q_2; Q_2; Q_2; \quad \mu_0' = 2 \end{aligned} \quad (9)$$

and we obtained the estimate $\mu_0' = 0.85J$. According to eq. 8, the chemical potential of magnons is renormalized $\mu_0' = \mu_0 - 2n$, and the low-energy magnons are hybridized due to the second term in eq. 8. This term shifts the bottom of the magnon band slightly down and leads to a weak mass enhancement of low-energy magnons. Both effects are proportional to n^2 and we omit them since $n \ll 1$ near T_c for $(B_c - B) \ll B_c$.

For a given $B \ll B_c$ and with decreasing temperature the magnon BEC occurs when the effective chemical potential μ_{eff} vanishes [6]. Then $T_c(B)$ is determined by

$$g_B(B_c - B) = 2n(T_c); \quad (10)$$

Here $n(T) = \sum_q f_B(E_q)$ with $f_B(E_q)$ being the Bose distribution function taken at $\mu_{\text{eff}} = 0$ and $E_q = E_q^A$ or $E_q = E_q^B$. This means that for $T < T_c$ the magnon condensate develops simultaneously at $q = Q_{1,2}$. It is worth emphasizing that at $\mu_{\text{eff}} \rightarrow 0$ the distribution function $f_B(E)$ diverges as $T \rightarrow E$ for $E \rightarrow 0$. Therefore, the low-energy 3D magnon spectrum, $E < E_c$, mainly contributes and drives the BEC transition. The phase boundary can be calculated using eq. 10. It gives a very good description of the experimental data near B_c (see inset to Fig. 4), but deviates strongly at lower fields, i.e., for $B_c - B > 0.5$ T. This indicates that the mean-field description of the magnon BEC is only applicable in the close vicinity of B_c . The calculated boundary is well described by eq. 1 with a critical exponent $\nu_{\text{th}} = 1.5$ close to the predicted value $\nu_{\text{BEC}} = 3/2$ characteristic for 3D quadratic dispersion of low-energy magnons [5, 6].

We have presented experimental evidence that in Cs_2CuCl_4 the field dependence of the critical temperature $T_c(B)/(B_c - B)^{\nu_{\text{th}}}$ is close to the critical field $B_c = 8.51$ T is well described with $\nu_{\text{th}} = 1.5$. This is in very good agreement with the exponent expected in the mean-field approximation. Together with the observed opening of a spin gap above B_c these findings support the notion of a Bose-Einstein condensation of magnons in Cs_2CuCl_4 .

We are grateful to D. Ihle, B. Schmidt, M. Sigrist, P. Thalmeier, Y. Tokiwa, and M. Vojta for stimulating discussions. V.Y. acknowledges financial support by the Deutsche Forschungsgemeinschaft.

- [3] R. Coldea et al., J. Phys.: Condens. Matter 8, 7473 (1996).
- [4] R. Coldea et al., Phys. Rev. Lett. 88, 137203 (2002).
- [5] O. Nohadani et al., Phys. Rev. B 69, 220402(R) (2004).
- [6] T. Nikuni et al., Phys. Rev. Lett. 84, 5868 (2000).
- [7] Ch. Ruegg et al., Nature 423, 62 (2003).
- [8] A. K. Kolezhuk et al., Phys. Rev. B 70, 020403(R) (2004).
- [9] H. Wilhelm et al., Rev. Sci. Instrum. 75, 2700 (2004).
- [10] The nuclear contributions were determined from a plot of $C_{\text{tot}}T^2$ vs T^3 , assuming that $C_{\text{tot}} = C_{\text{nuc}} + C_{\text{mag}} + C_{\text{ph}}$. The nuclear contributions are due to the hyperfine interactions and can be written as $C_{\text{nuc}} = \chi T^2 = (\chi_Q + \chi_Z)T^2$, with the quadrupolar and the Zeeman contribution, respectively. In this way we obtained $\chi_Q = 33(11)$ JK/mol and $\chi_Z = 13 \pm 3(3)B^2$ JK/(mol T^2). The latter value is in good agreement with the estimated value $\chi_Z = 11$ JK/mol, using NMR-data [11].
- [11] G. C. Carter et al., in Metallic shifts in NMR, Progress in Materials Science, ed. by B. Chalmers, J. W. Christian, and T. B. Massalski, Pergamon Press, Oxford, Vol. 20, Part I, Chap. 9, p.123-124 (1997).
- [12] A. Klumper, Eur. Phys. J. B 5, 677 (1998).
- [13] Z. Weihong, private communication.
- [14] R. Coldea et al., Phys. Rev. Lett. 86, 1335 (2001).
- [15] This can be achieved through $S_i^+ \rightarrow a_i$, $S_i^- \rightarrow a_i^\dagger$, and $S_i^z = 1/2 - a_i^\dagger a_i$, and a similar description for b_j .
- [16] M. Y. Veillette et al., cond-mat/0501347.
- [17] S. Bailleul et al., Eur. J. Solid State Inorg. Chem. 31, 431 (1994).
- [18] A. A. Abrikosov, L. G. Gorkov, and I. D. Zyaloshinskii, "Methods of quantum field theory in statistical physics" New York, Dover Publ. (1975).